Supplement of Atmos. Meas. Tech., 19, 63–78, 2026
https://doi.org/10.5194/amt-19-63-2026-supplement

Atmospheric Measurement Techniques
Open Access
EGU

Supplement of

Comparing spatial and temporal variabilities between the Vaisala AQT530 monitor and reference measurements

Roubina Papaconstantinou et al.

Correspondence to: George Biskos (g.biskos@cyi.ac.cy, g.biskos@tudelft.nl)

S.1 Technical information of sensors utilised

Table S1: Type and specifications of the reference instruments employed at the Nicosia traffic air quality monitoring station.

	CO	*NO_x*	*O_3*	*PM*
Model	Ecotech Serinus 30	Ecotech Serinus 40	Thermo Scientific 49i	TEOM Model: 1405-DF
Method	Absorption Spectroscopy	Chemiluminescence	Ultraviolet Photometry	Oscillating Microbalance
Sample flow rate	1.0 slpm	0.3 slpm (0.6 slpm total flow for the NO and NO_x flow path)	1–3 LPM	$PM_{2.5}$: 3 LPM, PM_{coarse} : 1.67 LPM, Bypass flow rate: 12 LPM
Precision	20 ppb or 0.1% of reading, whichever is greater	0.4 ppb otherwise 0.5% of reading, whichever is greater	–	± 2.0 μg/m³ (1-hour average)
Linearity	Better than ±1% of full scale (0-50 ppm); ±2% of full scale (0-200 ppm), from best straight-line fit	±1% of full scale	± 1% of full-scale	
Response time	60 seconds to 95%	15 seconds to 90%	20 seconds (10 seconds lag time)	
Lower detectable limit	40 ppb	0.4 ppb	1.0 ppb	< 5 μg/m^3

Table S2: Type and specifications of the reference instruments employed at CyI CAO air quality monitoring station.

	CO	*NO_2*	*O_3*	*PM*
Model	Teledyne Model T300	Teledyne Model T500U	Teledyne Model T400	TEOM Model: 1405-DF
Method	Absorption Spectroscopy	UV Fluorescence	UV Absorption	Oscillating Microbalance
Sample flow rate	800 cc/min ±10%	900 cc/min ±10%	800 cc/min ±10%	$PM_{2.5}$: 3 LPM, PM_{coarse} : 1.67 LPM, Bypass flow rate: 12 LPM
Precision	0.5% of reading above 5 ppm	0.5% of reading above 5 ppb	0.5% of reading above 100 ppb	± 2.0 μg/m³ (1-hour average)
Linearity	1% of full scale	1% of full scale	1% of full scale	
Response time	< 70 seconds to 95%	< 40 seconds to 95%	< 30 seconds to 95%	
Lower detectable limit	< 0.04 ppm	< 40 ppt	< 0.4 ppb with 80 Sample Digital Filter	< 5 μg/m^3

S.2 Data processing:

The reference measurements of the concentrations of the gaseous pollutants at TRS that are originally provided in μg/m^3 units are converted to ppb as follows:

$$C_{\text{gas}} = \rho_{gas} \times (273.2 + \text{T}))/(12.187 \times \text{M}),$$

where C_{gas} and ρ_{gas} are the concentrations in ppb and in μg/m^3, respectively, T is the temperature in °C and M is the molecular weight (in g/mol) of each gas. No further processing is applied on the data.

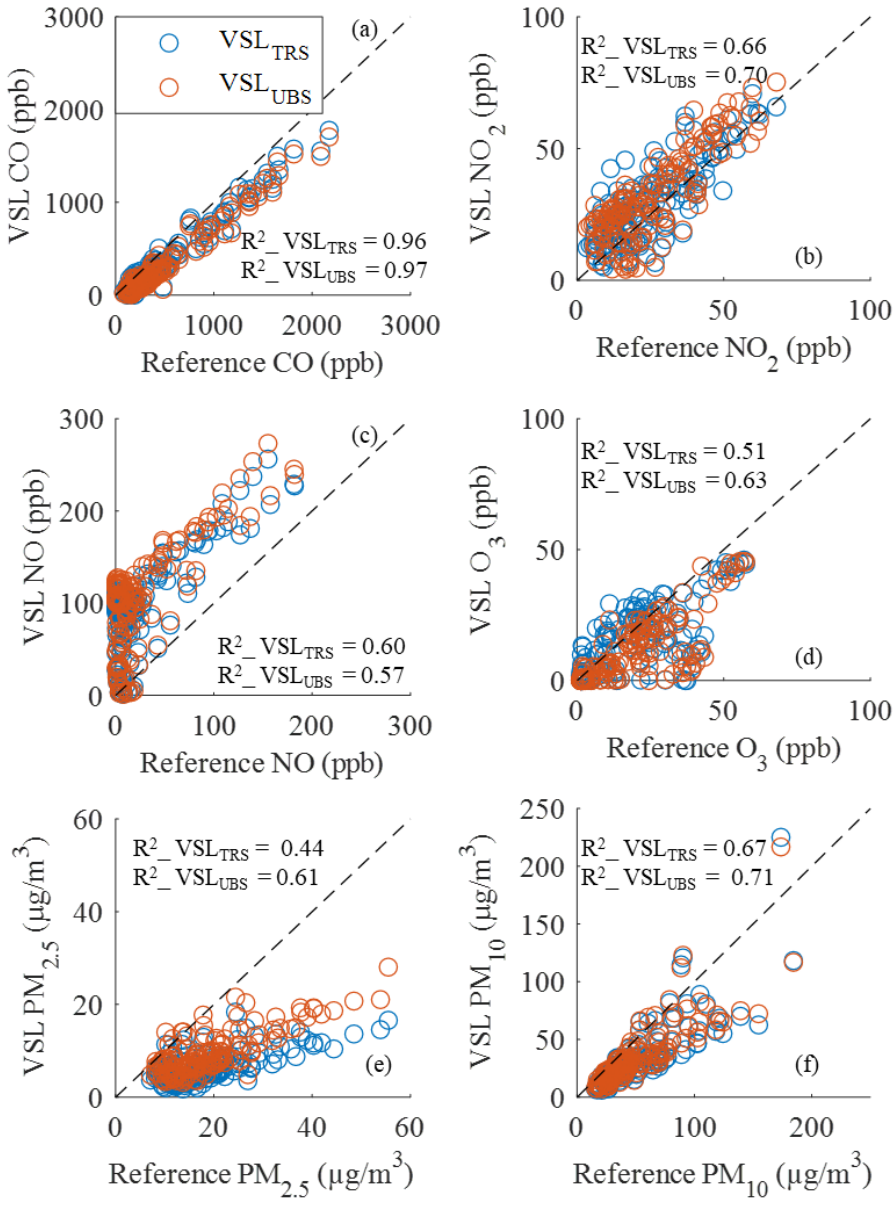

Figure S1: Correlation between hourly averaged measurements recorded by the VSL$_{\text{TRS}}$ (blue circles) and VSL$_{\text{UBS}}$ (red circles) sensors, with those provided by the respective reference instruments during the collocation week. The black dashed lines indicate the 1:1 relation.

S.3 Overall performance

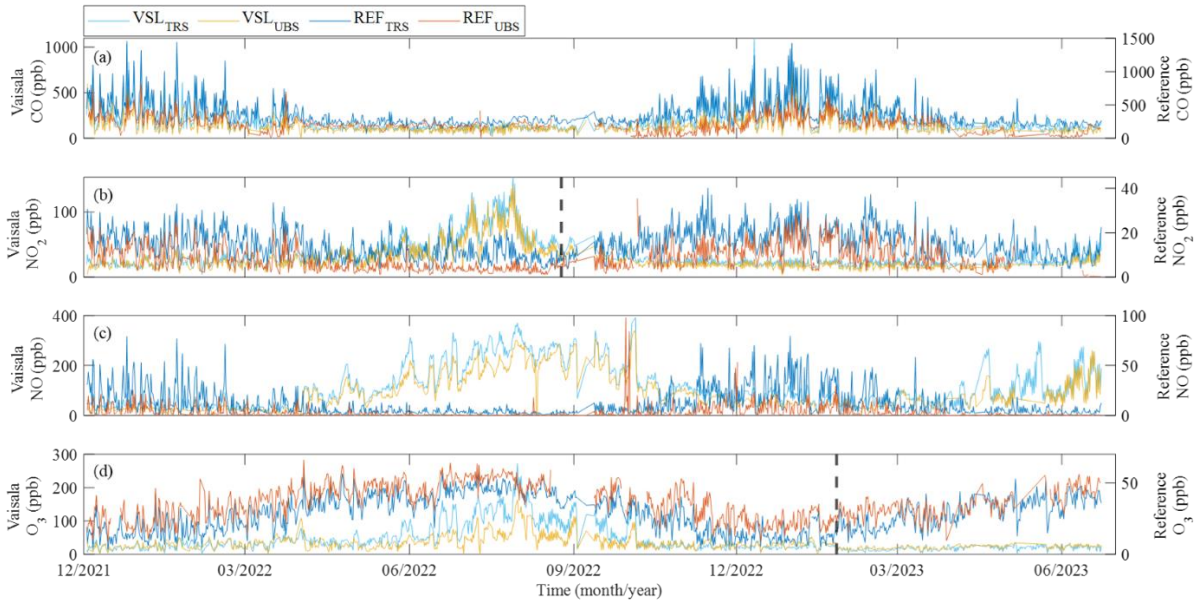

Figure S2: Time series of 12-hour averaged concentrations measured by the VSL_{TRS} and VSL_{UBS} gas sensors for CO (a), NO_2 (b), NO (c), and O_3 (d) over the entire measurement period. The VSL_{TRS} and VSL_{UBS} measurements are plotted on the left y-axis while the ones from the reference instruments (i.e., REF_{TRS}, REF_{UBS}) are plotted on the right y-axis. Black dashed lines indicate the time that the firmware was updated for the NO_2 (on 25/08/2022) and for the O_3 (on 26/01/2023) sensors.

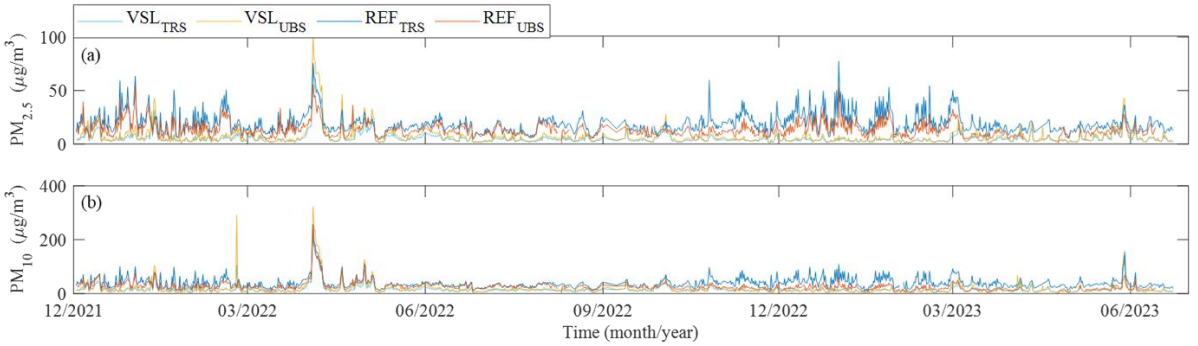

Figure S3: Time series of 12-hour averaged concentrations measured by the VSL_{TRS} and VSL_{UBS} PM sensors for the $PM_{2.5}$ (a) and the PM_{10} (b) mass fractions over the entire measurement period.

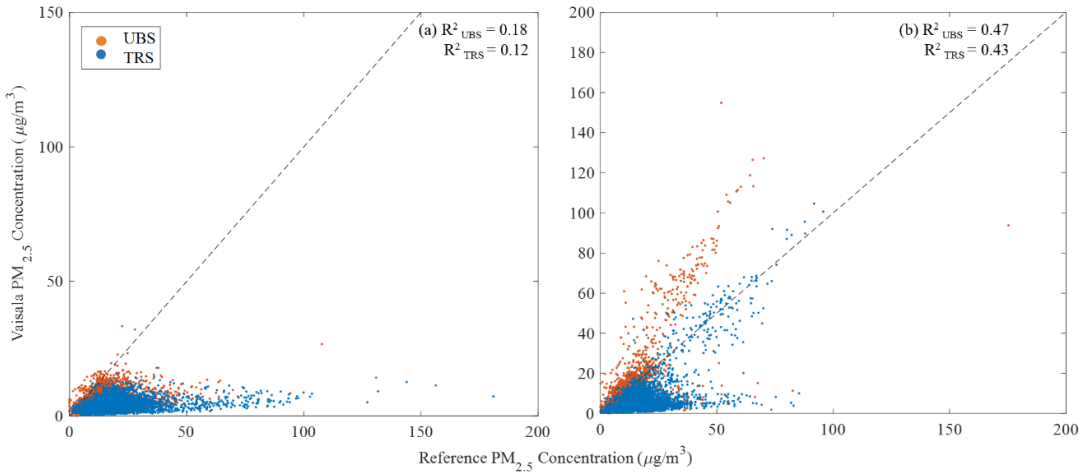

Figure S4: Correlation between hourly-averaged $PM_{2.5}$ measurements recorded by the AQTs at the two stations and those provided by the respective reference instruments during the non-dust periods (i.e., summer and winter; a) and dust periods (i.e. spring and autumn; b). The black dashed lines indicate the 1:1 relation.

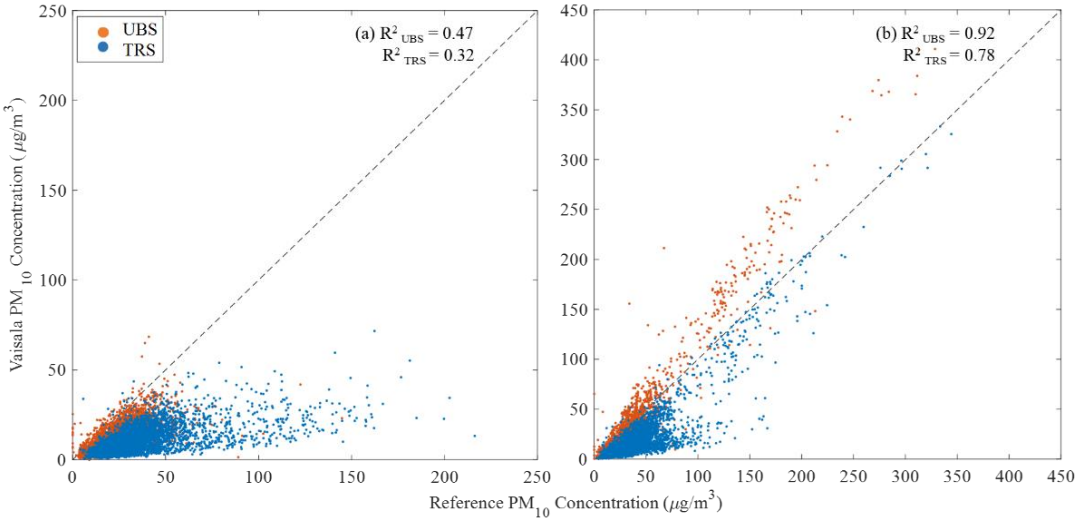

Figure S5: Correlation between hourly-averaged PM_{10} measurements recorded by the AQTs at the two stations and those provided by the respective reference instruments during the non-dust periods (i.e. summer and winter; a) and dust periods (i.e. spring and autumn; b). The black dashed lines indicate the 1:1 relation.

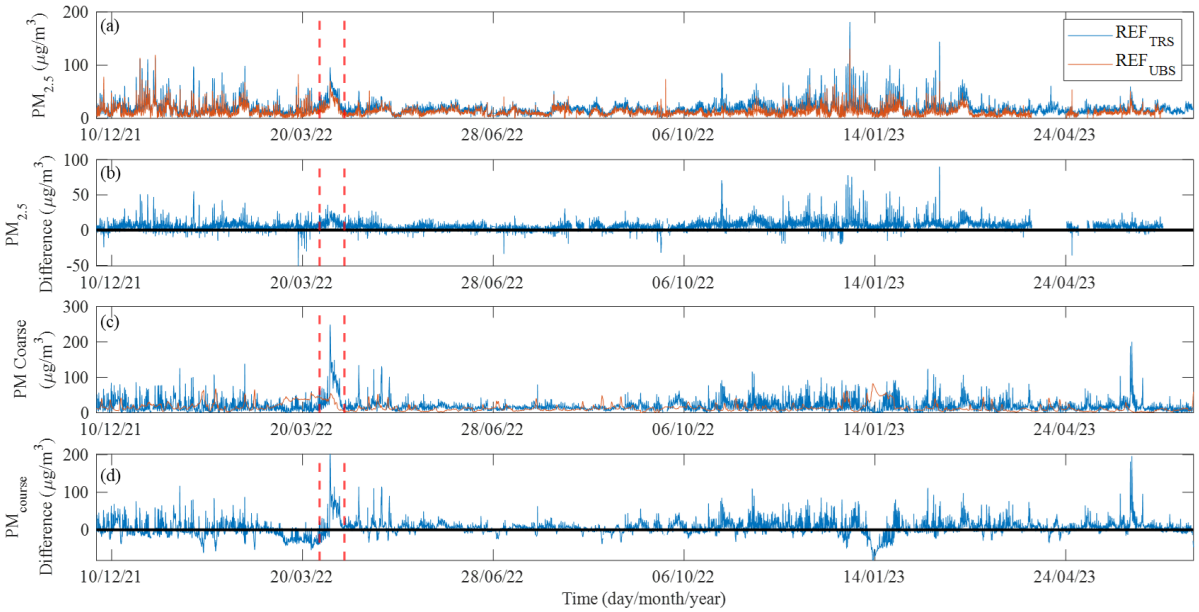

Figure S6: Time series of hourly-averaged $PM_{2.5}$ and coarse PM concentrations measured by the reference instruments at TRS and UBS. The differences in $PM_{2.5}$ and PM coarse between the two reference measurements are also plotted. The solid black line represents zero. Data between the red dashed lines indicate a major dust event in April 2022.

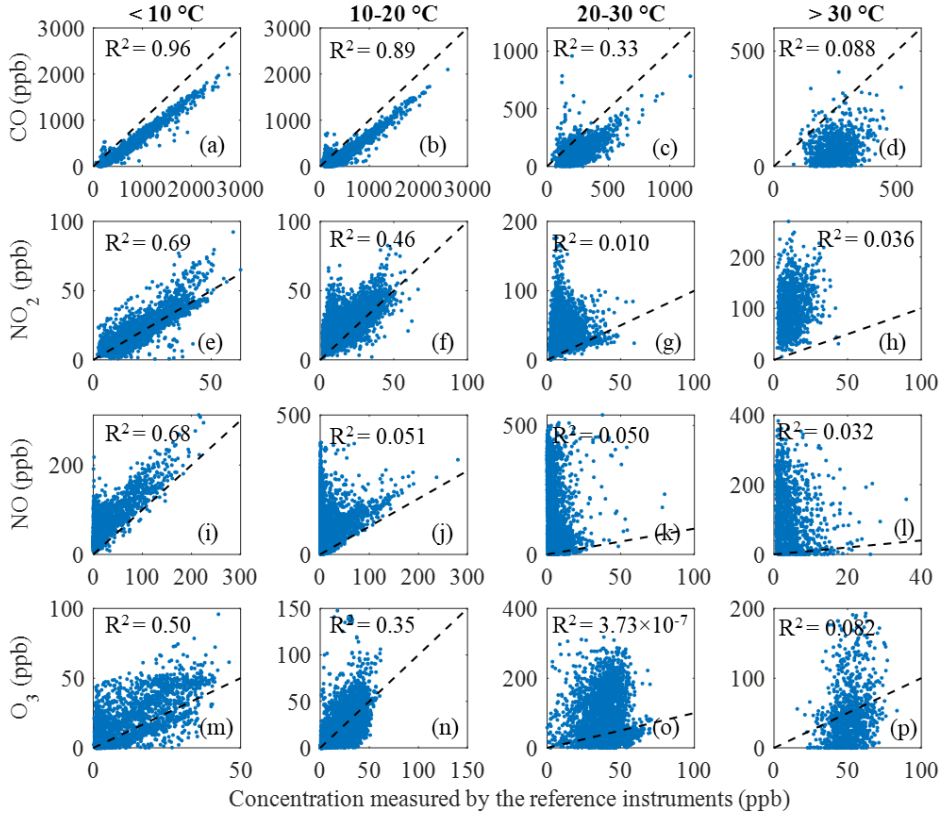

Figure S7: Correlation between the measurements recorded by the VSL_{TRS} gas sensors, and those provided by the respective reference instruments at four different temperature ranges. The 1:1 relations in each subplot are depicted as dashed lines.

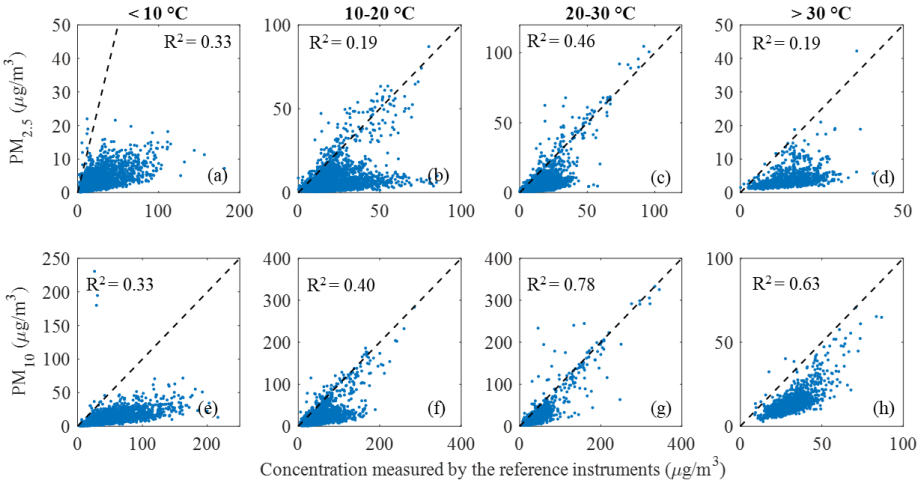

Figure S8: Correlation between the mass concentration measurements recorded by the VSL_{TRS} particle sensor, and those provided by the respective reference instruments at four different temperature ranges. The 1:1 lines in each subplot are depicted as dashed lines.

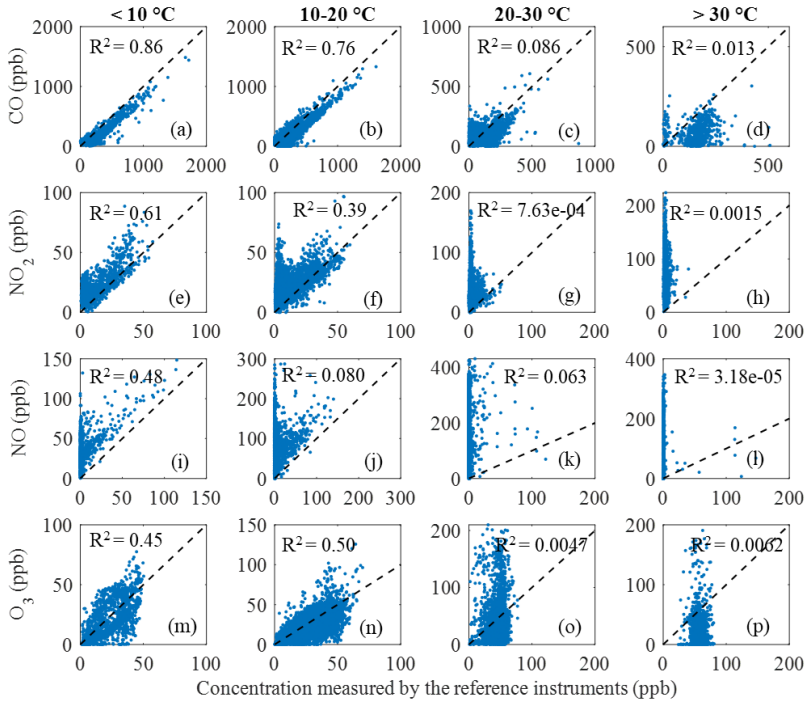

Figure S9: Correlation between the measurements recorded by the VSL_{UBS} gas sensors, and those provided by the respective reference instruments at four different temperature ranges. The 1:1 lines in each subplot are depicted as dashed lines.

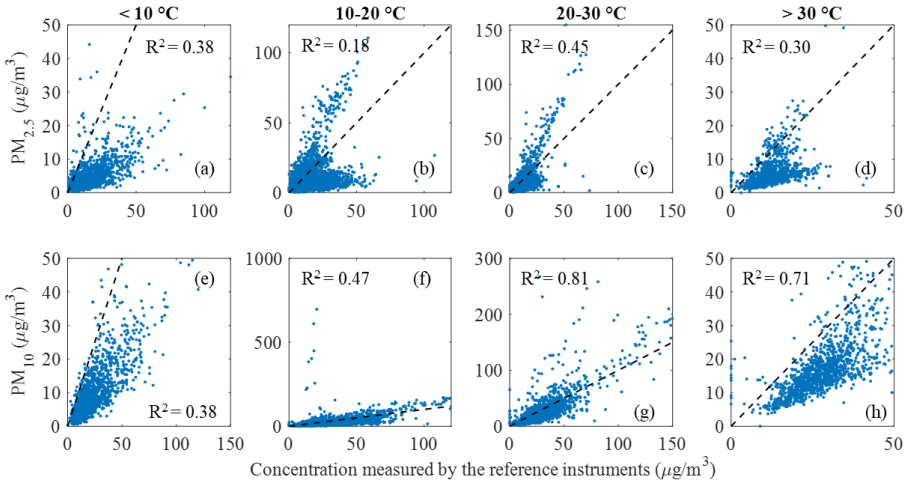

Figure S10: Correlation between the mass concentration measurements recorded by the VSL_{UBS} particle sensor, and those provided by the respective reference instruments at four different temperature ranges. The 1:1 lines in each subplot are depicted as dashed lines.

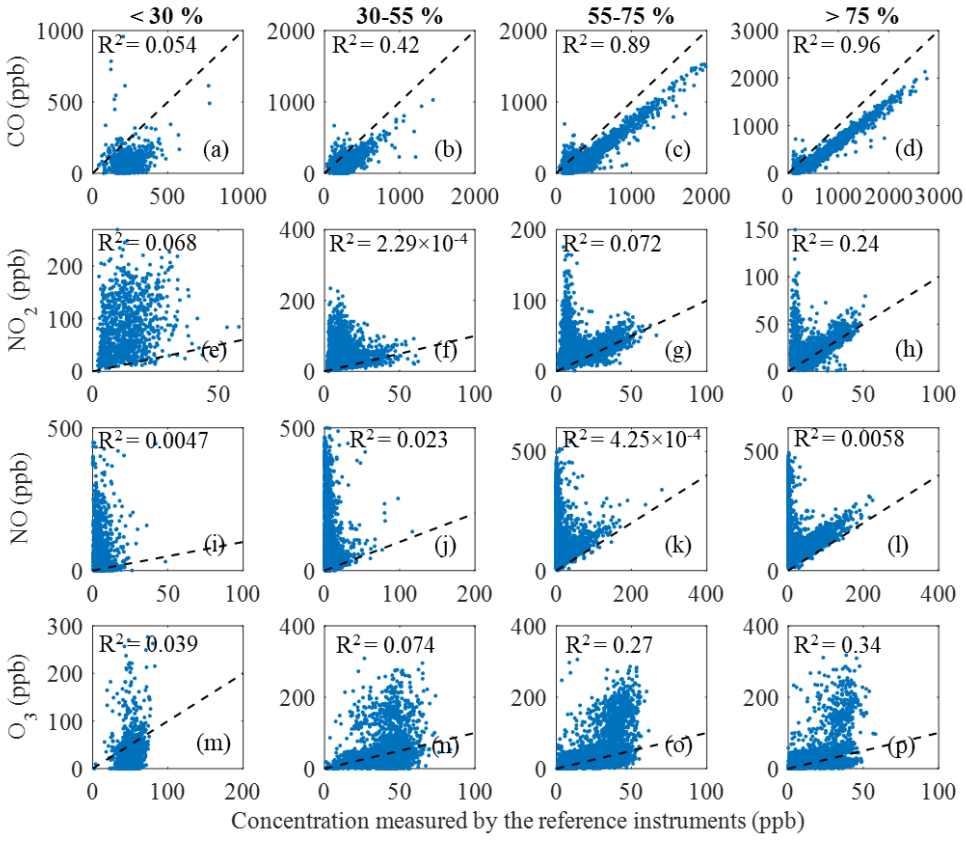

Figure S11: Correlation between the measurements recorded by the VSL_{TRS} gas sensors and those provided by the respective reference instruments at four different RH ranges. The 1:1 relations in each subplot are depicted as dashed lines.

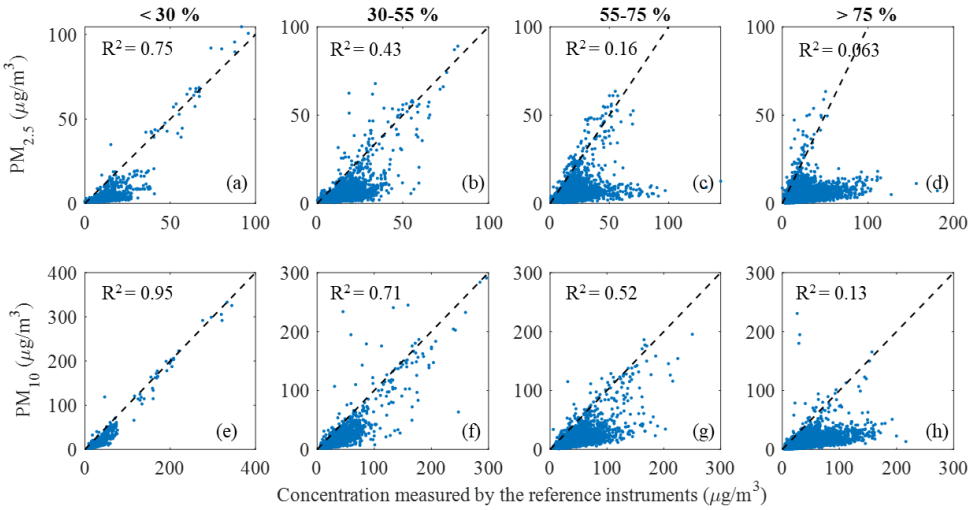

Figure S12: Correlation between the mass concentration measurements recorded by the VSL_{TRS} particle sensor, and those provided by the respective reference instruments at four different RH ranges. The 1:1 relations in each subplot are depicted as dashed lines.

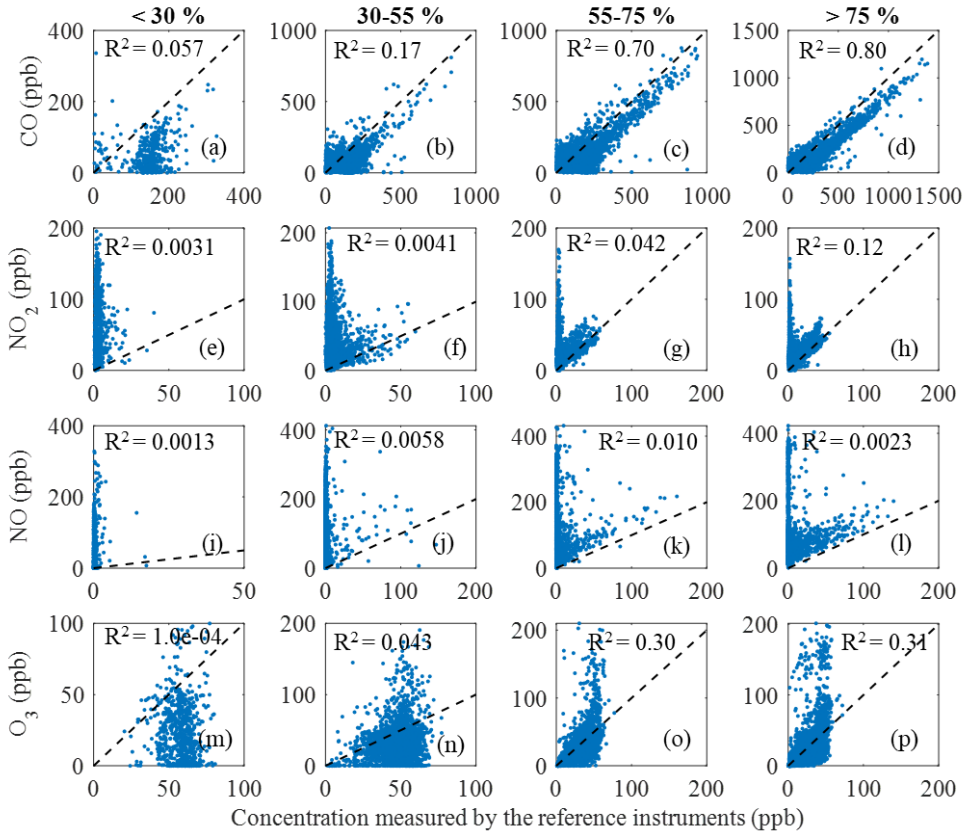

Figure S13: Correlation between the measurements recorded by the VSL_{UBS} gas sensors and those provided by the respective reference instruments at four different RH ranges. The 1:1 relations in each subplot are depicted as dashed lines.

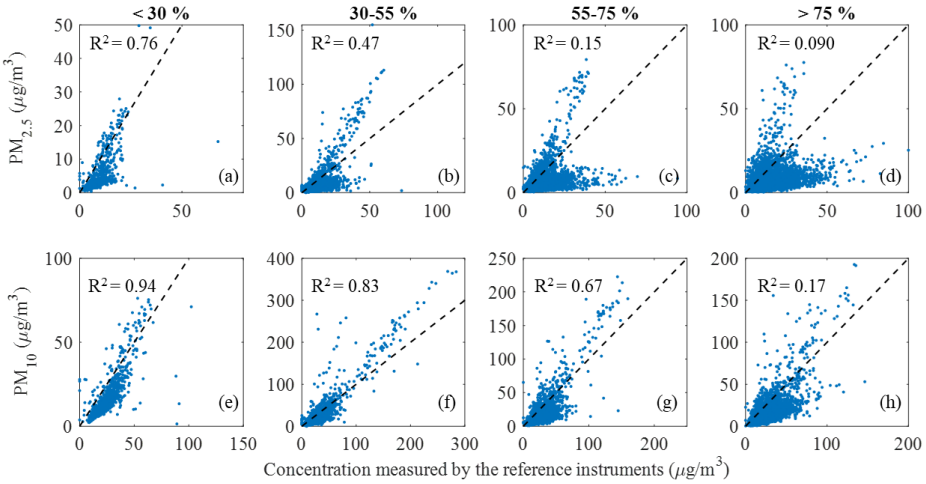

Figure S14: Correlation between the mass concentration measurements recorded by the VSL_{UBS} particle sensor and those provided by the respective reference instruments at four different RH ranges. The 1:1 relations in each subplot are depicted as dashed lines.

S.4 Significance of the difference between observations of the two stations

The Wilcoxon rank sum test method is a non-parametric test for two paired populations (*x*, *y*) assuming they are randomly and independently distributed. It returns the p-value for the null hypothesis that data in *x* and *y* are samples from continuous distributions with equal medians, against the alternative that they are not. The Wilcoxon rank sum test relies on the z-statistic defined as:

$$z = \frac{W - \frac{n(n+1)}{4}}{\sqrt{\frac{n(n+1)(2n+1)}{24}}},$$

where *n* is the sample size of the difference (*x* – *y*), and W is a parameter calculated by the following procedure: (1) determine the absolute difference between the two measurements ($|D_i|$), (2) assign ranks from 1 to *n* to each $|D_i|$ such that the smallest absolute difference is ranked as 1 and the largest as *n*, (3) reassign the symbol "+" or "–" to each of the *n* ranks, depending on whether D_i is originally positive or negative, (4) calculate the sum of the positive ranks (W+) and the sum of the negative ranks (W-), where W is the smallest value between W+ and W-. The calculated *z* value is then compared against a critical *z* value obtained from the so-called *z*-table. If the calculated *z* is less or equal to the critical *z* value, then the null hypothesis is rejected, implying a significant difference between the two populations (p value < 0.05).

Entire period

Table S3: Wilcoxon rank sum test results. In all cases, p values were < 0.05, indicating that the null hypothesis of the test is true.

	Reference measurements		AQT measurements	
	p value	Significant difference (p < 0.05)	p value	Significant difference (p < 0.05)
CO	0	true	9.9×10^{-142}	true
NO_2	0	true	3.8×10^{-99}	true
NO	0	true	3.3×10^{-68}	true
O_3	8.3×10^{-316}	true	7.0×10^{-12}	true
$PM_{2.5}$	0	true	7.9×10^{-117}	true
PM_{10}	0	true	2.0×10^{-14}	true

Monthly variabilities

Table S4: Wilcoxon rank sum test results for the CO measurements on a monthly basis. Bold underlined numbers indicate p values > 0.05, corresponding to cases where the null hypothesis of the test is rejected.

	Reference measurements		AQT measurements	
	p value	Significant difference ($p < 0.05$)	p value	Significant difference ($p < 0.05$)
Dec. 2021	1.1×10^{-17}	true	3.2×10^{-07}	true
Jan. 2022	1.9×10^{-36}	true	1.9×10^{-11}	true
Feb. 2022	4.1×10^{-68}	true	1.8×10^{-10}	true
Mar. 2022	2.2×10^{-96}	true	1.6×10^{-12}	true
Apr. 2022	3.2×10^{-52}	true	1.0×10^{-06}	true
May 2022	1.3×10^{-57}	true	4.4×10^{-05}	true
Jun. 2022	1.3×10^{-26}	true	3.2×10^{-04}	true
Jul. 2022	1.6×10^{-30}	true	5.2×10^{-01}	**false**
Aug. 2022	5.5×10^{-89}	true	6.8×10^{-01}	**false**
Sept. 2022	1.3×10^{-84}	true	6.7×10^{-05}	true
Oct. 2022	2.6×10^{-142}	true	3.5×10^{-11}	true
Nov. 2022	4.4×10^{-126}	true	1.0×10^{-19}	true
Dec. 2022	1.1×10^{-44}	true	1.8×10^{-16}	true
Jan. 2023	3.0×10^{-48}	true	3.1×10^{-15}	true
Feb. 2023	3.3×10^{-73}	true	8.3×10^{-25}	true
Mar. 2023	1.3×10^{-17}	true	9.3×10^{-14}	true
Apr. 2023	1.1×10^{-163}	true	5.2×10^{-14}	true
May 2023	1.9×10^{-121}	true	1.0×10^{-17}	true
Jun. 2023	1.4×10^{-92}	true	2.5×10^{-12}	true

Table S5: Wilcoxon rank sum test results for all PM_{10} measurements on a monthly basis. Bold underlined numbers indicate p values > 0.05, corresponding to cases where the null hypothesis of the test is rejected.

	Reference measurements		AQT measurements	
	p value	Significant difference ($p < 0.05$)	p value	Significant difference ($p < 0.05$)
Dec. 2021	5.6×10^{-14}	true	4.2×10^{-01}	**false**
Jan. 2022	3.5×10^{-18}	true	7.2×10^{-02}	true
Feb. 2022	3.8×10^{-29}	true	7.0×10^{-01}	**false**
Mar. 2022	1.2×10^{-35}	true	3.1×10^{-01}	**false**
Apr. 2022	2.8×10^{-06}	true	1.0×10^{-07}	true
May 2022	1.4×10^{-06}	true	3.3×10^{-15}	true
Jun. 2022	5.2×10^{-09}	true	1.0×10^{-14}	true
Jul. 2022	8.8×10^{-05}	true	4.0×10^{-29}	true
Aug. 2022	1.2×10^{-31}	true	4.4×10^{-34}	true
Sept. 2022	1.5×10^{-36}	true	3.2×10^{-07}	true
Oct. 2022	2.8×10^{-77}	true	1.5×10^{-06}	true
Nov. 2022	2.8×10^{-133}	true	7.2×10^{-02}	**false**
Dec. 2022	2.3×10^{-121}	true	1.4×10^{-03}	true
Jan. 2023	1.2×10^{-69}	true	4.6×10^{-03}	true
Feb. 2023	6.3×10^{-98}	true	3.4×10^{-09}	true
Mar. 2023	2.4×10^{-132}	true	4.3×10^{-01}	**false**
Apr. 2023	1.6×10^{-87}	true	3.7×10^{-01}	**false**
May 2023	4.2×10^{-129}	true	6.2×10^{-01}	**false**
Jun. 2023	9.1×10^{-64}	true	1.5×10^{-04}	true

Hour-of-the-day (diurnal) variabilities

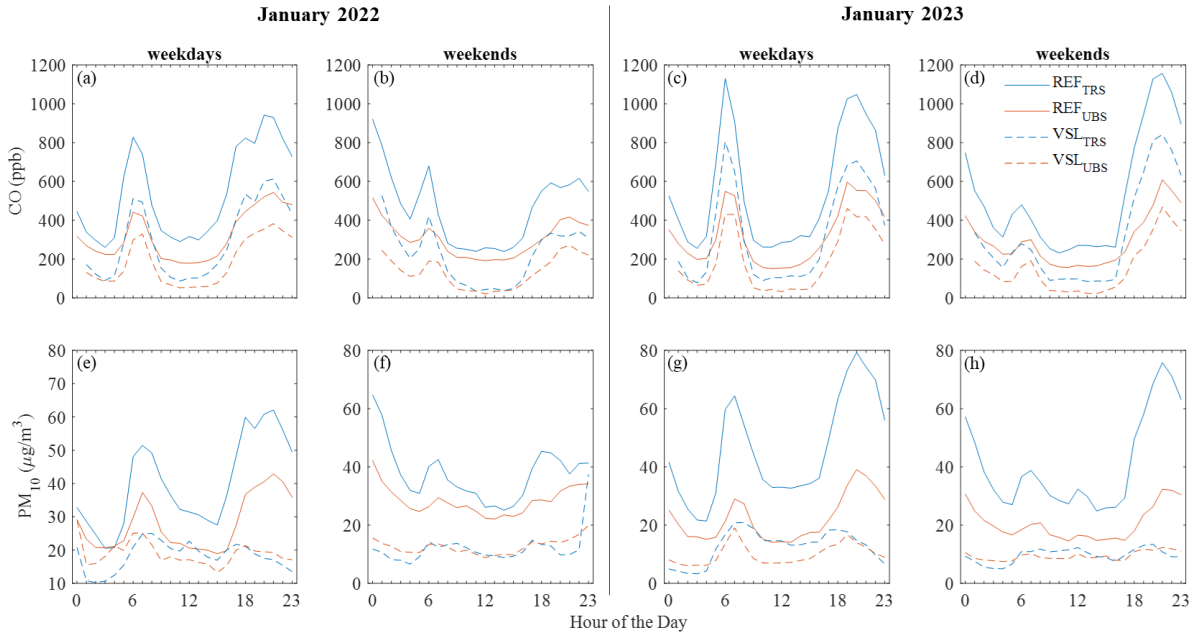

Figure S15: Diurnal variability of the hourly-averaged CO (a-d) and PM_{10} (e-h) concentration measurements in January 2022 (left column) and January 2023 (right column) determined by the reference instruments (solid lines) and the Vaisala AQT sensors (dashed lines) at the two stations. The blue and orange lines correspond to measurements at TRS and UBS stations, respectively.

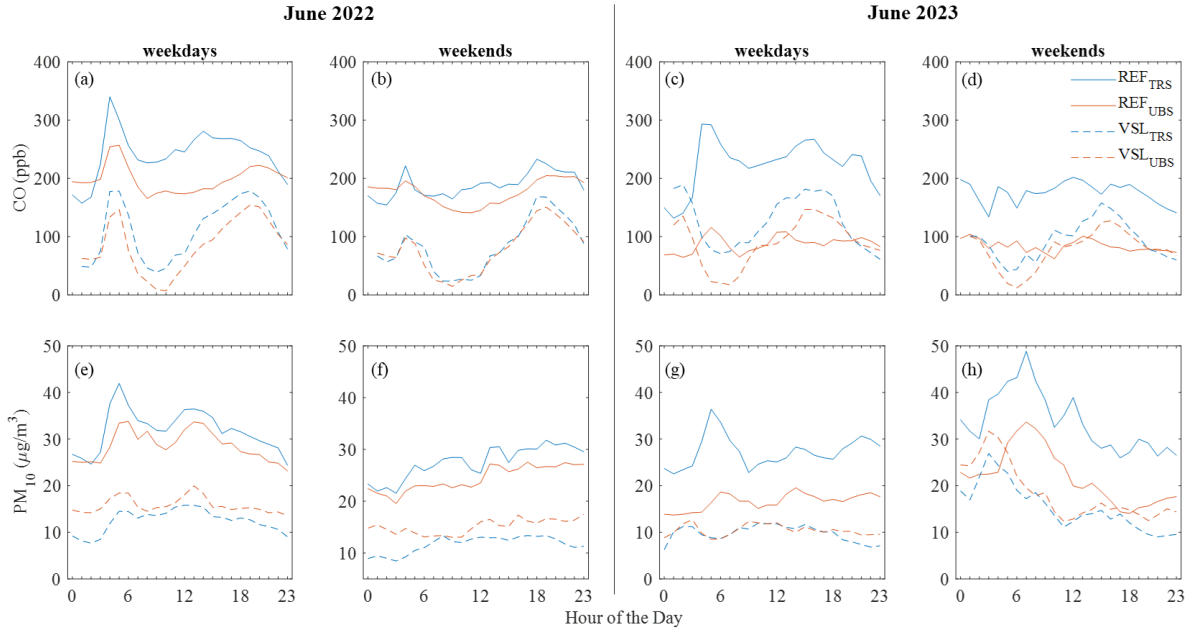

Figure S16: Diurnal variability of the hourly-averaged CO (a-d) and PM_{10} (e-h) measurements in June 2022 (left column) and June 2023 (right column) determined by the reference instruments (solid lines) and the Vaisala AQT sensors (dashed lines) at the two stations. The blue and orange lines correspond to measurements at TRS and UBS stations, respectively.

Table S6: Wilcoxon rank sum test results for all CO measurements. Bold underlined numbers indicate p values > 0.05, corresponding to cases where the null hypothesis of the test is rejected.

	Reference measurements				AQT measurements			
	June 2022 - 2023		January 2022 - 2023		June 2022 - 2023		January 2022 - 2023	
	p value		p value		p value		p value	
Hour	workdays	weekends	workdays	weekends	workdays	weekends	workdays	weekends
0	$\underline{\mathbf{5.6 \times 10^{-01}}}$	$\underline{\mathbf{7.3 \times 10^{-01}}}$	2.1×10^{-02}	$\underline{\mathbf{9.6 \times 10^{-02}}}$	$\underline{\mathbf{2.3 \times 10^{-01}}}$	$\underline{\mathbf{3.5 \times 10^{-01}}}$	$\underline{\mathbf{3.0 \times 10^{-01}}}$	$\underline{\mathbf{1.9 \times 10^{-01}}}$
1	$\underline{\mathbf{9.7 \times 10^{-02}}}$	$\underline{\mathbf{8.7 \times 10^{-01}}}$	$\underline{\mathbf{1.6 \times 10^{-01}}}$	$\underline{\mathbf{1.2 \times 10^{-01}}}$	$\underline{\mathbf{6.9 \times 10^{-01}}}$	$\underline{\mathbf{8.4 \times 10^{-01}}}$	$\underline{\mathbf{4.9 \times 10^{-01}}}$	$\underline{\mathbf{1.9 \times 10^{-01}}}$
2	$\underline{\mathbf{4.6 \times 10^{-01}}}$	$\underline{\mathbf{9.5 \times 10^{-01}}}$	$\underline{\mathbf{5.2 \times 10^{-02}}}$	$\underline{\mathbf{1.4 \times 10^{-01}}}$	$\underline{\mathbf{4.9 \times 10^{-01}}}$	$\underline{\mathbf{6.6 \times 10^{-01}}}$	$\underline{\mathbf{8.5 \times 10^{-01}}}$	$\underline{\mathbf{3.2 \times 10^{-01}}}$
3	2.1×10^{-02}	$\underline{\mathbf{7.7 \times 10^{-01}}}$	1.3×10^{-02}	$\underline{\mathbf{3.7 \times 10^{-01}}}$	1.2×10^{-02}	$\underline{\mathbf{6.6 \times 10^{-01}}}$	$\underline{\mathbf{8.5 \times 10^{-01}}}$	$\underline{\mathbf{1.9 \times 10^{-01}}}$
4	4.8×10^{-07}	$\underline{\mathbf{3.5 \times 10^{-01}}}$	2.0×10^{-06}	$\underline{\mathbf{9.0 \times 10^{-02}}}$	1.7×10^{-03}	$\underline{\mathbf{8.9 \times 10^{-01}}}$	2.5×10^{-03}	$\underline{\mathbf{1.5 \times 10^{-01}}}$
5	2.5×10^{-06}	$\underline{\mathbf{4.8 \times 10^{-01}}}$	1.9×10^{-09}	7.1×10^{-04}	2.5×10^{-02}	$\underline{\mathbf{5.1 \times 10^{-01}}}$	9.9×10^{-07}	1.3×10^{-03}
6	3.9×10^{-06}	$\underline{\mathbf{8.3 \times 10^{-01}}}$	5.9×10^{-07}	2.2×10^{-03}	8.8×10^{-06}	8.9×10^{-03}	1.4×10^{-04}	2.9×10^{-03}
7	1.5×10^{-08}	$\underline{\mathbf{1.0 \times 10^{-01}}}$	7.9×10^{-05}	3.3×10^{-02}	9.9×10^{-08}	1.0×10^{-02}	1.1×10^{-02}	4.1×10^{-02}
8	1.6×10^{-10}	$\underline{\mathbf{6.9 \times 10^{-02}}}$	2.1×10^{-06}	$\underline{\mathbf{5.8 \times 10^{-02}}}$	6.4×10^{-04}	$\underline{\mathbf{8.5 \times 10^{-01}}}$	5.3×10^{-04}	3.3×10^{-02}
9	5.0×10^{-08}	$\underline{\mathbf{1.3 \times 10^{-01}}}$	1.8×10^{-10}	1.7×10^{-02}	1.9×10^{-02}	$\underline{\mathbf{5.7 \times 10^{-01}}}$	7.5×10^{-07}	9.4×10^{-03}
10	3.4×10^{-08}	3.3×10^{-02}	1.6×10^{-10}	1.5×10^{-02}	$\underline{\mathbf{1.0 \times 10^{-01}}}$	$\underline{\mathbf{7.5 \times 10^{-01}}}$	1.4×10^{-03}	7.9×10^{-03}
11	7.7×10^{-08}	2.4×10^{-03}	8.3×10^{-12}	4.2×10^{-03}	4.5×10^{-03}	$\underline{\mathbf{8.9 \times 10^{-01}}}$	1.1×10^{-03}	$\underline{\mathbf{2.5 \times 10^{-01}}}$
12	3.7×10^{-07}	2.4×10^{-03}	7.7×10^{-12}	1.5×10^{-04}	7.1×10^{-03}	$\underline{\mathbf{8.2 \times 10^{-01}}}$	1.2×10^{-04}	2.9×10^{-02}
13	8.5×10^{-07}	6.1×10^{-03}	4.5×10^{-11}	2.1×10^{-04}	3.5×10^{-03}	$\underline{\mathbf{1.3 \times 10^{-01}}}$	1.0×10^{-04}	$\underline{\mathbf{6.5 \times 10^{-02}}}$
14	2.0×10^{-07}	1.9×10^{-02}	2.2×10^{-10}	4.6×10^{-04}	7.1×10^{-04}	$\underline{\mathbf{4.0 \times 10^{-01}}}$	8.6×10^{-05}	3.9×10^{-02}
15	5.0×10^{-09}	$\underline{\mathbf{1.4 \times 10^{-01}}}$	8.6×10^{-08}	2.4×10^{-03}	4.1×10^{-04}	$\underline{\mathbf{3.2 \times 10^{-01}}}$	8.2×10^{-06}	$\underline{\mathbf{6.2 \times 10^{-02}}}$
16	1.6×10^{-09}	1.6×10^{-02}	5.8×10^{-07}	3.7×10^{-04}	5.8×10^{-04}	$\underline{\mathbf{5.1 \times 10^{-01}}}$	8.2×10^{-05}	1.6×10^{-02}
17	6.2×10^{-09}	5.3×10^{-03}	2.7×10^{-05}	9.1×10^{-05}	2.2×10^{-04}	$\underline{\mathbf{2.4 \times 10^{-01}}}$	5.2×10^{-04}	1.3×10^{-03}
18	1.5×10^{-08}	1.2×10^{-02}	9.9×10^{-05}	5.1×10^{-03}	6.0×10^{-04}	$\underline{\mathbf{2.6 \times 10^{-01}}}$	2.5×10^{-03}	2.1×10^{-02}
19	6.8×10^{-05}	$\underline{\mathbf{2.1 \times 10^{-01}}}$	4.5×10^{-03}	1.0×10^{-02}	$\underline{\mathbf{7.4 \times 10^{-02}}}$	$\underline{\mathbf{3.7 \times 10^{-01}}}$	$\underline{\mathbf{8.6 \times 10^{-02}}}$	$\underline{\mathbf{6.4 \times 10^{-02}}}$
20	9.6×10^{-05}	$\underline{\mathbf{3.0 \times 10^{-01}}}$	2.5×10^{-04}	2.0×10^{-02}	$\underline{\mathbf{4.7 \times 10^{-01}}}$	$\underline{\mathbf{8.0 \times 10^{-01}}}$	1.1×10^{-02}	$\underline{\mathbf{7.5 \times 10^{-02}}}$
21	3.9×10^{-03}	$\underline{\mathbf{4.8 \times 10^{-01}}}$	2.2×10^{-03}	3.8×10^{-02}	$\underline{\mathbf{8.9 \times 10^{-01}}}$	$\underline{\mathbf{5.8 \times 10^{-01}}}$	3.3×10^{-02}	$\underline{\mathbf{1.7 \times 10^{-01}}}$
22	$\underline{\mathbf{5.3 \times 10^{-02}}}$	$\underline{\mathbf{6.6 \times 10^{-01}}}$	7.3×10^{-04}	$\underline{\mathbf{8.5 \times 10^{-02}}}$	$\underline{\mathbf{6.8 \times 10^{-01}}}$	$\underline{\mathbf{7.0 \times 10^{-01}}}$	1.5×10^{-02}	$\underline{\mathbf{2.4 \times 10^{-01}}}$
23	$\underline{\mathbf{6.7 \times 10^{-01}}}$	$\underline{\mathbf{8.0 \times 10^{-01}}}$	9.5×10^{-03}	$\underline{\mathbf{1.1 \times 10^{-01}}}$	$\underline{\mathbf{5.8 \times 10^{-02}}}$	$\underline{\mathbf{7.5 \times 10^{-01}}}$	$\underline{\mathbf{1.5 \times 10^{-01}}}$	$\underline{\mathbf{2.8 \times 10^{-01}}}$

Table S7: Wilcoxon rank sum test results for all PM_{10} measurements. Bold underlined cells indicate p values > 0.05, corresponding to cases where the null hypothesis of the test is rejected.

	Reference measurements				AQT measurements			
	June 2022 - 2023		January 2022 - 2023		June 2022 - 2023		January 2022 - 2023	
	p value		p value		p value		p value	
Hour	workdays	weekends	workdays	weekends	workdays	weekends	workdays	weekends
0	3.7×10^{-02}	2.1×10^{-01}	3.0×10^{-02}	2.3×10^{-02}	3.9×10^{-03}	9.4×10^{-02}	5.7×10^{-02}	4.1×10^{-01}
1	1.0×10^{-01}	2.7×10^{-01}	1.3×10^{-02}	2.9×10^{-02}	2.6×10^{-02}	1.5×10^{-01}	5.1×10^{-03}	$\mathbf{6.4 \times 10^{-01}}$
2	1.6×10^{-01}	1.6×10^{-01}	7.6×10^{-03}	8.5×10^{-02}	4.1×10^{-03}	1.2×10^{-01}	5.6×10^{-04}	5.0×10^{-02}
3	1.5×10^{-02}	1.4×10^{-01}	8.1×10^{-02}	1.7×10^{-01}	2.2×10^{-03}	9.4×10^{-02}	1.4×10^{-03}	4.7×10^{-02}
4	1.7×10^{-04}	1.2×10^{-01}	3.4×10^{-02}	1.6×10^{-01}	7.0×10^{-02}	1.2×10^{-01}	3.5×10^{-02}	7.0×10^{-02}
5	1.1×10^{-04}	1.1×10^{-01}	2.9×10^{-04}	9.6×10^{-02}	3.8×10^{-01}	3.2×10^{-01}	1.3×10^{-01}	3.4×10^{-01}
6	5.5×10^{-03}	2.3×10^{-01}	4.3×10^{-06}	3.8×10^{-03}	1.4×10^{-01}	$\mathbf{8.4 \times 10^{-01}}$	4.7×10^{-01}	$\mathbf{6.2 \times 10^{-01}}$
7	4.1×10^{-02}	1.3×10^{-01}	5.5×10^{-05}	1.7×10^{-02}	3.8×10^{-01}	$\mathbf{1.0 \times 10^{+00}}$	$\mathbf{5.7 \times 10^{-01}}$	$\mathbf{1.0 \times 10^{+00}}$
8	1.8×10^{-02}	2.5×10^{-01}	4.7×10^{-05}	7.5×10^{-02}	$\mathbf{9.7 \times 10^{-01}}$	$\mathbf{1.0 \times 10^{+00}}$	6.0×10^{-03}	3.7×10^{-01}
9	7.7×10^{-02}	3.2×10^{-01}	2.4×10^{-08}	5.4×10^{-02}	2.1×10^{-01}	$\mathbf{8.4 \times 10^{-01}}$	3.6×10^{-06}	1.9×10^{-01}
10	3.4×10^{-02}	2.5×10^{-01}	2.1×10^{-08}	1.1×10^{-01}	$\mathbf{6.6 \times 10^{-01}}$	$\mathbf{5.7 \times 10^{-01}}$	7.2×10^{-06}	3.1×10^{-01}
11	3.2×10^{-02}	8.5×10^{-02}	9.5×10^{-09}	5.0×10^{-02}	$\mathbf{9.4 \times 10^{-01}}$	$\mathbf{6.3 \times 10^{-01}}$	3.7×10^{-06}	2.8×10^{-01}
12	1.4×10^{-01}	9.5×10^{-02}	1.2×10^{-09}	6.2×10^{-02}	$\mathbf{6.8 \times 10^{-01}}$	4.0×10^{-01}	1.1×10^{-05}	3.6×10^{-01}
13	2.8×10^{-01}	1.3×10^{-01}	6.8×10^{-08}	2.9×10^{-02}	4.9×10^{-01}	$\mathbf{6.1 \times 10^{-01}}$	3.4×10^{-05}	4.5×10^{-01}
14	1.1×10^{-01}	1.3×10^{-01}	7.8×10^{-07}	2.3×10^{-01}	$\mathbf{8.3 \times 10^{-01}}$	4.8×10^{-01}	1.2×10^{-04}	$\mathbf{8.5 \times 10^{-01}}$
15	1.1×10^{-01}	2.1×10^{-01}	5.2×10^{-06}	1.4×10^{-01}	$\mathbf{9.6 \times 10^{-01}}$	4.0×10^{-01}	1.9×10^{-03}	$\mathbf{9.1 \times 10^{-01}}$
16	1.3×10^{-01}	1.1×10^{-01}	8.6×10^{-08}	4.0×10^{-02}	$\mathbf{8.5 \times 10^{-01}}$	2.6×10^{-01}	8.1×10^{-03}	$\mathbf{9.5 \times 10^{-01}}$
17	3.6×10^{-02}	2.1×10^{-01}	6.3×10^{-06}	1.7×10^{-02}	3.3×10^{-01}	4.0×10^{-01}	2.4×10^{-01}	$\mathbf{5.2 \times 10^{-01}}$
18	2.5×10^{-02}	1.7×10^{-01}	7.4×10^{-05}	7.8×10^{-03}	$\mathbf{5.7 \times 10^{-01}}$	1.6×10^{-01}	2.6×10^{-01}	$\mathbf{7.3 \times 10^{-01}}$
19	2.5×10^{-03}	6.0×10^{-02}	1.2×10^{-03}	3.1×10^{-02}	2.0×10^{-01}	1.5×10^{-01}	$\mathbf{8.4 \times 10^{-01}}$	$\mathbf{7.5 \times 10^{-01}}$
20	5.5×10^{-03}	5.4×10^{-02}	1.9×10^{-03}	1.0×10^{-01}	2.9×10^{-02}	1.0×10^{-01}	$\mathbf{9.7 \times 10^{-01}}$	$\mathbf{8.5 \times 10^{-01}}$
21	2.9×10^{-03}	1.6×10^{-01}	2.5×10^{-03}	1.4×10^{-01}	2.8×10^{-02}	2.6×10^{-02}	$\mathbf{9.9 \times 10^{-01}}$	4.3×10^{-01}
22	8.1×10^{-03}	1.4×10^{-01}	3.1×10^{-04}	1.5×10^{-01}	1.8×10^{-02}	1.6×10^{-02}	$\mathbf{5.5 \times 10^{-01}}$	4.8×10^{-01}
23	2.0×10^{-02}	3.4×10^{-01}	4.6×10^{-04}	2.2×10^{-01}	6.2×10^{-03}	2.0×10^{-02}	1.8×10^{-01}	$\mathbf{7.0 \times 10^{-01}}$